TOSHKENT DAVLAT TRANSPORT UNIVERSITETI
Tashkent state transport university

Issue 2, 2023

INTERNATIONAL JOURNAL OF TRANSPORT AND TECHNOLOGICAL MACHINES

ISSN: 3030-363X



THE SCIENCE OF TODAY IS THE TECHNOLOGY OF TOMORROW

TOSHKENT DAVLAT TRANSPORT UNIVERSITETI
Tashkent state transport university

INTERNATIONAL JOURNAL OF TRANSPORT AND TECHNOLOGICAL MACHINES

Published since 2023

Editorial Council:
Mukhitdinov A.A., Ziyayev K.Z., Rustamov K.J, Abdurazzakov U.
Editorial team:
Chief Editor – Rustamova N.R.
Deputy Chief Editor – Rustamov K.J.

Members of the editorial board:
Mukhitdinov A.A., Ziyayev K.Z., Rustamov K.J., Abdurazzoqov U.A., Saman M. Almufti., Habibollah Haron., Gai-ge Wang., Jayson A. Dela Fuente., Ahmad A. AlRabab'ah., Rami Hikmat Fouad AL-Hadeethi., Emad Kamil Hussein., Ayman Abu-Rumman.

TASHKENT STATE TRANSPORT UNIVERSITY

Founder of the scientific and technical journal, “International Journal of Transport and Technological Machines” – Tashkent State Transport University (100167, Republic of Uzbekistan, Tashkent, Temiryulchilar str., house No. 1, office: 379, tel Tel.: +998 97 156 94 21 E-mail: k.j.rustamov82@gmail.com).

In the International Journal of Transport and Technological Machines publishes the most significant results of scientific and applied research carried out in universities of transport and information technology profile, other higher educational institutions, research institutes and centers of the Republic of Uzbekistan and foreign countries.

The journal is published 4 times a year and contains publications in the following main areas:

- Automotive engineering
- Civil Engineering
- Construction Engineering and Management
- Instrumentation technology
- Environmental Engineering
- Environmental Sciences
- Green production
- Industrial Safety
- Mechanical Engineering Technology
- Mining
- Mechatronics

CONTENTS

1. Riskulov A.A., Antonov A.S. ENGINEERING MATERIALS BASED ON MODIFIED INDUSTRIAL THERMOPLASTICS..... 4
2. Khankelov T.K., Politaeva N. A. RESULTS OF EXPERIMENTAL STUDIES OF THE PROCESS OF CRUSHING ORGANIC COMPONENTS OF MUNICIPAL SOLID WASTE..... 13

ENGINEERING MATERIALS BASED ON MODIFIED INDUSTRIAL THERMOPLASTICS

Riskulov A.A.[1], Antonov A.S.[2]

[1]Tashkent State Transport University, Tashkent, Uzbekistan
[2]Yanka Kupala State University of Grodno, Grodno, Belarus

Abstract. The mechanisms of formation of the structure of polymer blends with different thermodynamic compatibility of components are considered. A synergistic effect was obtained to increase the parameters of performance characteristics and resistance to thermal-oxidative degradation during the formation of products and functional coatings from industrial polymer blends through the use of plasticizers that increase the segmental mobility of macromolecules in the temperature range of formation of the product and coating, and low-dimensional (including nano-sized) particles of various compositions , structure and production technology, acting as a physical compatibilizer. Nanocomposite materials based on thermoplastics blends have been developed for the manufacture of products and coatings used in the construction of automobile components, technological tool, belt conveyor, fastening elements, elements of road and construction structures.

Keywords: polymer blends, composite material, composite structure, physical compatibilizer, functional coating.

1. Introduction

Modern mechanical engineering is characterized by an increase in the proportion of functional materials based on industrially produced polymeric and oligomeric binders due to the developed technologies for modifying their structure in order to achieve optimal parameters of stress-strain, tribological, adhesive, etc. characteristics and effective methods of their production and processing into products [1].

Currently, there are a number of effective directions for managing the parameters of the structural characteristics of industrial binders by introducing functional fillers and components into their composition that affect the mechanisms of formation of supramolecular structures, the mechanisms of intermolecular interaction, the kinetics of the course of thermo-oxidative and destructive processes, etc. in the static and dynamic interaction of products made of functional materials with a metal coupled element [1, 2]. At the same time, the development of machine-building production, the improvement of the service system of operated equipment, increased attention to the impact of polymer composites in their production, processing into products and their operation on environmental components put forward new tasks to improve the technology of functional materials based on polymer and oligomeric matrices.

In the applied areas of mechanical engineering, a special place is occupied by composite materials based on blends of industrially produced materials, which have a developed base for their production and processing, which significantly reduces the cost of manufacturing and operating functional products.

The purpose of this work was to study the main directions of formation of functional materials with high performance characteristics based on industrially produced thermoplastics.

2. Research methodology

Industrially produced thermoplastic polymers of the class of polyamides (PA 6, PA 6.6, PA 11, PA 12), polyolefins (HDPE, LDPE, PP), polyacetals (copolymer of formaldehyde and

1,3-dioxolane (FDO), polyoxymethylene (POM)), polyesters (PET, PBTF), thermoplastic elastomers (thermoplastic polyurethane (TPU), ethylene-vinyl acetate (EVA) copolymer, divinyl styrene thermoplastic elastomer (DST), microcellular polyesterurethane (MPEU)) produced by Belarus enterprises (Filial "Plant Khimvolokno" JSC "Grodno Azot", Plant "Polymir" JSC "Naftan", JSC "Mogilevkhimvolokno") or Russian and Uzbekistan enterprises were selected for research.

To modify the basic polymers (matrix binders), a developed injection molding technology was used, which is most widely used in mechanical engineering to obtain functional products.

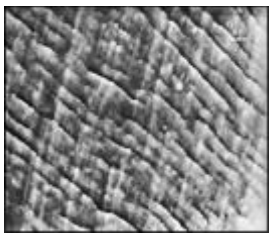
As modifiers of matrix binders, both thermoplastic compounds and dispersed particles of carbon-containing (ultradispersed detonation diamond (UDD), thermally expanded graphite (TEG), colloidal graphite C-1), metal-containing (Cu, Zn, Ni), silicon-containing (clay) components were used.

Analysis of the thermophysical parameters of composite materials was carried out by the DTA method on the Thermoscan-2. The study of the structural features of the materials obtained was carried out by IR spectroscopy (IR Fourier microscope Nicolet iN 10), atomic force microscopy (atomic force microscope NT-206), scanning electron microscopy (SEM microscope JEOL JSM-5610 LV with electron-probe energy dispersion X-ray microanalyzer EDX JED-2201). The parameters of the stress-strain characteristics of composites were evaluated on standard samples according to generally accepted methods.

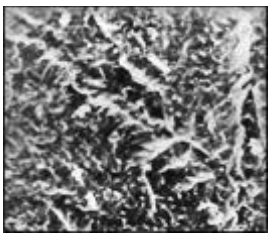
3. Results and discussion

In the formation of the structure of composite materials based on the blends of thermoplastic components, the most significant contribution is made by the parameters of the molecular structure and mass, which determine the thermophysical, stress-strain and rheological characteristics of the matrix and modifying polymer, which form the basis of their thermodynamic compatibility.

When combining components with a similar structure of the molecular chain and a molecular weight of the same order, the rheological characteristics of the matrix and modifying polymer are of decisive importance in the formation of the structure of the composite with the necessary and sufficiently stable parameters of performance characteristics. The difference in viscosity leads to the formation of a heterophase structure of various types. When a high-viscosity polymer (FDO, DST, TPU, HDPE, ABS) is introduced into a low-viscosity (PA 6, PP), a heterogeneous structure is formed with a pronounced separation of the phases of the alloying component in the matrix binder [2]. Dispersed fragments of the modifier melt under the action of shear stresses during rotation of the mixer screw are distributed in a low-viscosity matrix with formation of a characteristic structure. With such a combination, the formation of interfacial layers at the boundary of the "matrix – modifier" section is fragmentary in nature and does not determine the values of the performance characteristics (tensile strength σ_{uts}, impact strength α, compressive strength σ_c) (Fig. 1).



(a)



(b)

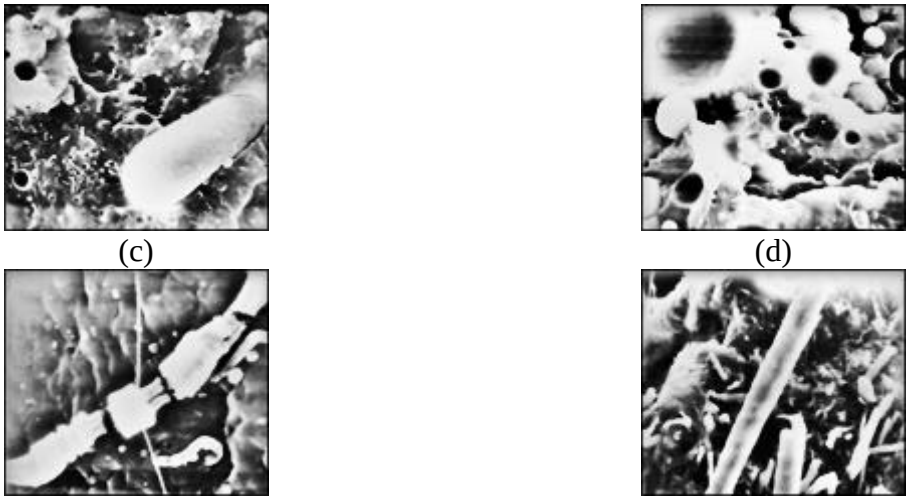


Fig. 1. Characteristic type of chips in liquid nitrogen (a–d) and fracture surfaces after uniaxial stretching (e, f) of samples from PA 6 (a), FDO (b), compositions PA 6 + 5 wt. % FDO (c, e) and PA 6+50 wt. % FDO (d, f). 100×

Dispersed fragments of a modifying polymer with a size of 10–150 μm perform the function of a reinforcing (FDO, ABS) or structural modifier that reduces residual stresses in a composite sample due to pronounced chain flexibility and a lower melting point (TPU, DST, HDPE). The degree of dispersion of the alloying polymer in the matrix polymer is determined mainly by the mixing parameters (temperature, time, intensity (speed) of the screw movement) and the ratio of the components. At the ratios of matrix polymer : modifier 1 : 0.01–0.10, a fairly homogeneous heterophase structure is formed with high parameters of performance characteristics (Fig. 2) [2].

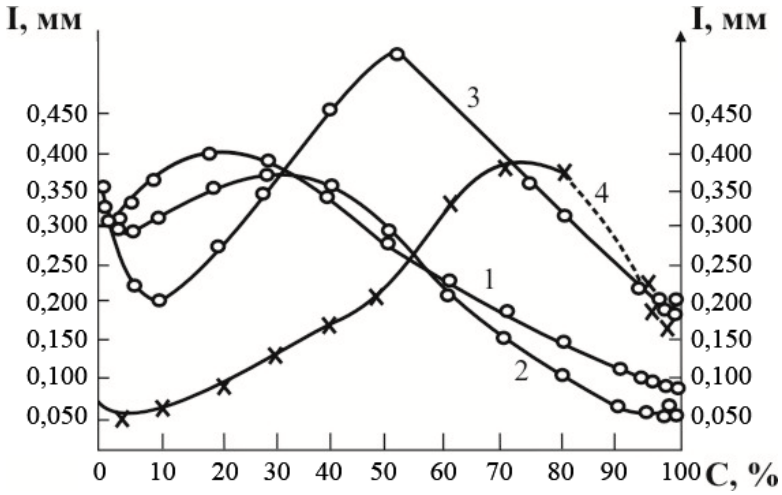


Fig. 2. Dependence of the wear intensity of FDO (1–3) and PA 6 (1) on the content of MPEU (1), TPU (2) and DST (3, 4)

The content of the phase formed by the mechanochemical interaction of the components with the formation of a copolymer product is insignificant. Nevertheless, there was an increase in the parameters of the thermophysical characteristics of mixed composites of this type (activation energy $E_{act.}$, heat resistance, resistance to thermal oxidative destruction) due to the destruction of

weak areas of macromolecules in the process of thermomechanical action and the formation of copolymer products [2–4].

When a relatively low-viscosity modifier (PA 6, FDO, ABS) is introduced into a highly viscous matrix (TPU, DST, MPEU), a heterophase structure with a high degree of homogeneity is formed, a characteristic feature of which is the formation of modifying elements of various shapes and sizes. Relatively viscous modifiers (ABS, FDO) form fragments in the matrix binder (TPU, DST, MPEU) in the size range of 1–120 μm with pronounced localization (Fig. 3). These fragments, the size of which depends on the ratio of the matrix and alloying components have a predominantly spherical shape, due, obviously, to the correlation of melting points (transition to a viscous-fluid state).

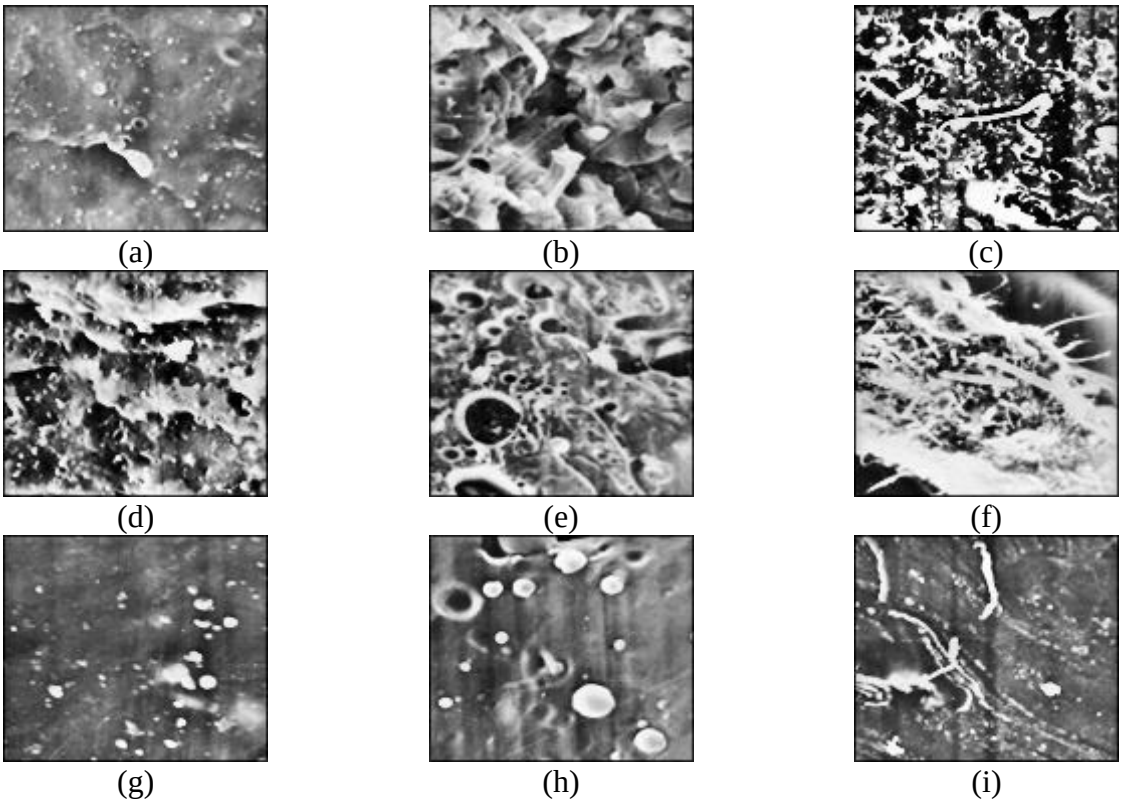


Fig. 3. Characteristic appearance of the surface of chips in liquid nitrogen and fracture surfaces after uniaxial stretching of samples based on DST (a, b, c), MPEU (d, e, f), TPU (g, h, i), modified 5 wt. % PA 6 (c), 5 wt. % FDO (e), 50 wt. % PA 6 (f) and 50 wt. % FDO (h). 100×

In the composite "high-viscosity polymer (DST) – low-viscosity modifier (PA 6)" the formation of alloying component aggregates of a predominantly arbitrary shape is observed, due to the low viscosity of the PA 6 melt and the possibility of its dispersion when combining components in screw mixers. The intensity of thermomechanical action on the mixture DST – PA 6 significantly affects the parameters of stress-strain and thermophysical characteristics [2, 3].

Blends of thermodynamically incompatible polymers PA 6 – FDO, PA 6 – HDPE, PA 6 – DST, TPU – FDO, TPU – ABS, HDPE – ABS, HDPE – FDO in the field of ratios of matrix and alloying components 1 : 0.01–0.10 wt. %. are characterized by a heterophase structure with a

sufficiently high macrohomogenicity, which determines the increased values of the parameters of their stress-strain, tribological, adhesive characteristics [2].

Materials can be obtained using common screw mixers without the use of special functional components that regulate compatibility parameters – compatibizers. Thermomechanical combination is intensified by introducing low-molecular plasticizers (petroleum and vegetable oils, tars, etc.) into the composition [2]. With thermomechanical combination of matrix and alloying components with a similar structure of the molecular chain and the value of the molecular weight - aliphatic polyamides (PA 6, PA 6.6, PA 11, PA 12), polyolefins (PP, HDPE, LDPE, EVA), fluoroplastics (polytetrafluoroethylene (PTFE), ultradispersed polytetrafluoroethylene (UPTFE), fluorine-containing oligomers) – a heterophase structure with increased homogeneity is formed. The close structure of the molecular chain, correlating molecular weight values create the prerequisites for the correlation of the rheological characteristics of the melts of the matrix and alloying components.

When the elements of the mixer are exposed to a mixture of melts of the components, they are dispersed to form a structure with a transition layer formed as a result of the interdiffusion of macromolecules with a similar molecular structure and segmental mobility, which provides increased thermodynamic compatibility of the matrix and alloying components with the formation of a three-phase system – "matrix polymer – transition layer – alloying polymer". Such composites are a combination of the copolymer phase formed as a result of the interaction of radical products of thermo- and mechanodestruction, and a mixture of macromolecules formed as a result of the interdiffusion of macromolecules of the matrix and alloying components with similar values of molecular weight, molecular chain structure and segmental mobility. The presence of a transition layer creates the prerequisites for the implementation of the characteristic features of each component in the composite material – stress-strain, thermophysical, energy, adhesive characteristics.

When combining aliphatic polyolefins with various thermophysical parameters (melting point T_m, oxidation temperature T_{ox}, destruction temperature T_d) and a similar molecular structure of polyamides PA 6, PA 6.6 with PA 11, PA 12, it is possible to implement two characteristic features. Alloying of high-melting polyamide (PA 6, PA 6.6) with low-melting (PA 11, PA 12) allows to reduce residual stresses in the sample (or coating) due to the preservation of the liquid-phase state of the alloying component after matrix crystallization. For example, in the system PA 6 (PA 6.6) + PA 11 (PA 12), the crystallization processes of the matrix occur in the temperature range of 180–200 °C while maintaining the melt phase of the alloying component. After reaching a temperature of 140–160 °C, the crystal structure of the composite is cooled, at which the crystalline component of the modifier retains increased deformability, acting as a stabilizer of shrinkage processes that reduces residual stresses in the sample or coating.

The experimentally considered mechanism of influence of a low-melting modifier in the PA 6 (PA 6.6) – PA 11 (PA 12) system is confirmed by an increase in the parameters of the deformation and strength characteristics of the composite compared to the characteristics of the matrix polymer when introduced into the composition of a component with deliberately lower values of parameters σ_{uts}, σ_c, E, tribological and the adhesive characteristics of composite coatings on metal substrates (Tables 1 and 2, Fig. 4) [4].

Table 1. Parameters of stress-strain characteristics of blends based on the aliphatic polyamides (testing for stretching)

Composite material, wt. %	Parameter characteristics				
	σ_m, MPa	ε_m, %	σ_b, MPa	ε_b, %	ε_{fb}, %

PA6.6(94%)+PA6(5%)+PA12(1%)	77,71	4,3	53,4	–	23,60
PA6.6(90%)+PA6(5%)+PA12(5%)	75,58	5,9	49,0	23	20,87

Table 2. Parameters of deformation-strength chemicals of composite materials based on mixtures of aliphatic polyamides (testing for exposure)

Composite material, wt. %	Parameter characteristics				
	σ_m, MPa	ε_m, %	σ_b, MPa	ε_b, %	ε_{fb}, %
PA6,6(84,5%)+PA6(10%)+PA12(5%)+ colloidal graphite C1(0,5%)	78,84	3,9	76,0	3,8	6,3
PA6.6(84.5%)+PA6(10%)+PA12(5%)+ carbon nanotubes (CNT) (0.5%)	54,19	2,1	54,2	2,1	–
PA6,6(84,5%)+PA6(10%)+PA12(5%)+UDD(0.5%)	77,78	3,8	74,1	3,7	12

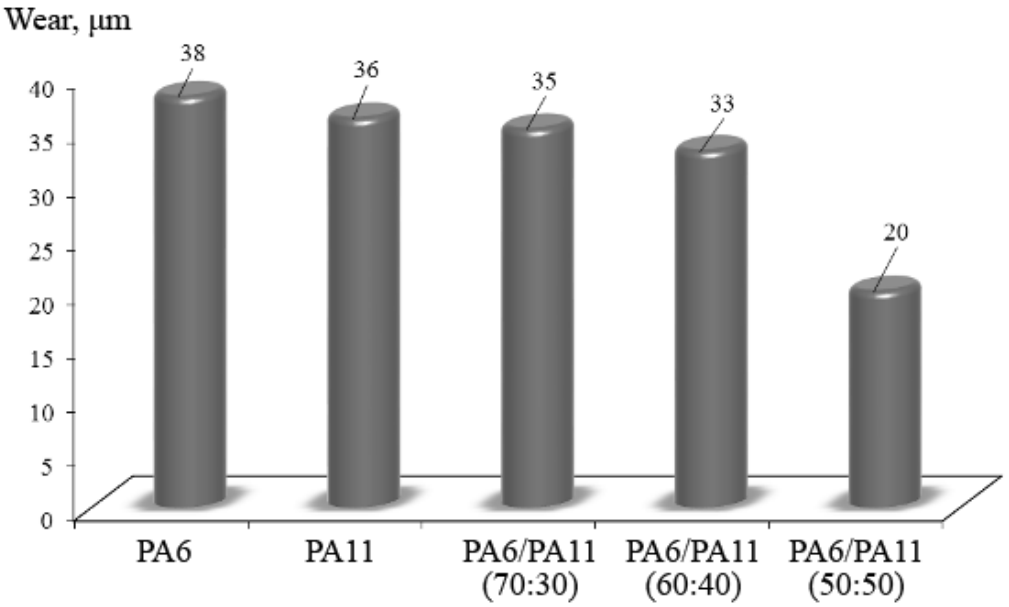


Fig. 4. Wear resistance of polyamide coatings under friction without external lubrication

Similar effects were noted for compositions PA 6.6 – PA 6, PP – HDPE, PP – LDPE, HDPE – LDPE [4, 6].

When a high-melting modifier with a close molecular chain structure is introduced into a matrix polymer with a lower melting point due to thermomechanical combination in the range of temperatures exceeding the melting point of the modifier, a system is formed in which the alloying component performs the function of a reinforcing additive. Due to the close values of molecular weight and rheological characteristics, a transition layer is formed in the system, which ensures the compatibility of components and the formation of a heterogeneous structure with increased parameters of stress-strain and tribological characteristics. Composites of LDPE – HDPE, LDPE – PP, HDPE – PP, EVA – PP, PA 6 – PA 6.6, PA 11 (PA 12) – PA 6 (PA 6.6) are superior in parameters to σ_{uts}, σ_c, Brinell hardness *HB* matrix binders due to the reinforcement of components with increased strength. A characteristic feature of such composites is the possibility of forming products not only with thermomechanical combination using screw mixers or injection molding machines with a screw plasticizer, but also coatings for various purposes

(protective, decorative, tribological, insulating) by deposition from fluidized bed or gas-thermal spraying [4].

Additional effects in the formation of products and functional coatings from blends of thermodynamically compatible polymers can be achieved by using plasticizers that increase the segmental mobility of macromolecules in the range of temperatures of product formation and coating, and low-dimensional (including nanoscale)) particles of different composition, structure and production technology that change the mechanisms of interphase interactions at the interface of the "matrix – modifier" section due to the formation of physical connections of the adsorption type with the active centers of the matrix and alloying components (Fig. 5) [5].

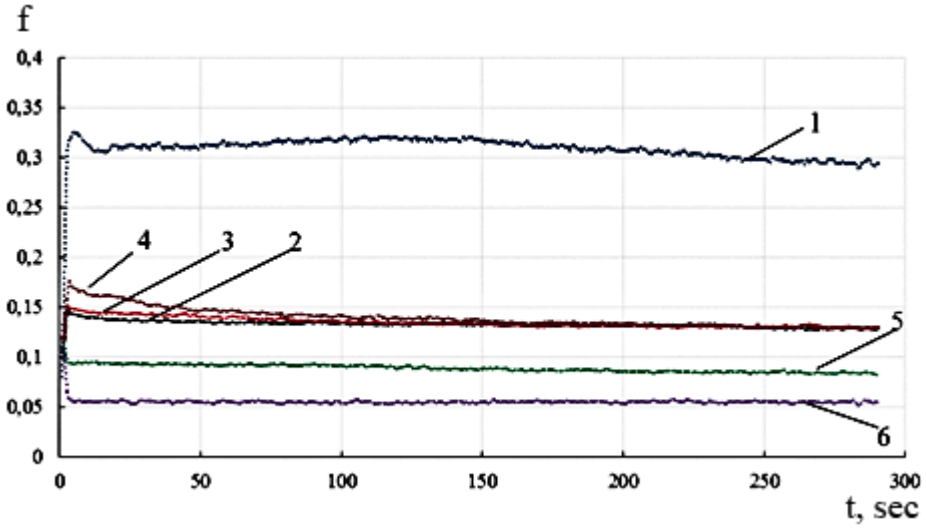


Fig. 5. Dependence of the coefficient of friction on the operating time for coatings from composite materials based on aliphatic polyamides:
1 – PA 6; 2 – PA 11; 3 – PA 6/PA 11 (50:50) + 0,1 wt. % C-1;
4 – PA 6/PA 11 (50:50) + 0,5 wt. % C-1;
5 – PA 6/PA 11 (50:50) + 0,1 wt. % CNT;
6 – PA 6/PA 11 (50:50) + 0,5 wt. % CNT

Low-dimensional particles that exhibit nanostration due to size, structure or energy treatment perform the function of regulators of rheological characteristics due to the formation of both intra- and intermolecular bonds, including intermolecular bonds in the boundary layer [4, 5]. This leads not only to an increase in the parameters of deformation and strength characteristics, but also resistance to thermo-oxidizing destruction (Fig. 6).

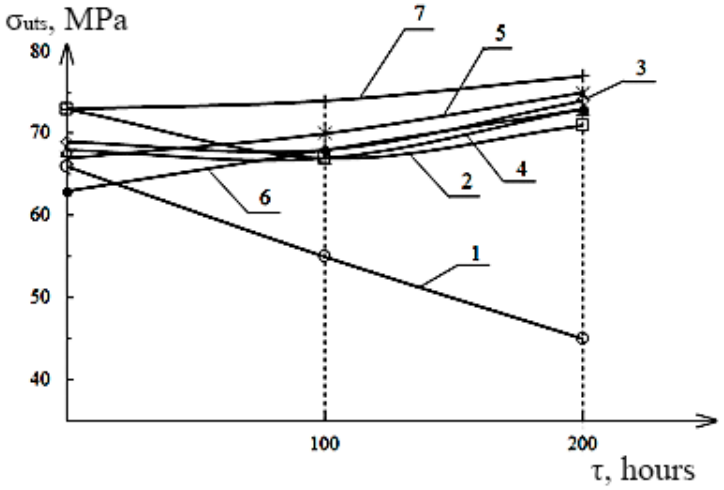


Fig. 6. Dependence of the strength dimension at contraction from the thermal oxidation time at 150 °C:
1 – PA 6.6; 2 – PA6.6 (94 wt. %) + PA6 (5 wt. %) + PA12 (1 wt. %);
3 – PA6.6 (90 wt. %) + PA6 (5 wt. %) + PA12 (5 wt. %);
4 – PA6,6 (85 wt. %) + PA6 (10 wt. %) + PA12 (5 wt. %);
5 – PA6.6 (84.5 wt. %) + PA6 (10 wt. %) + PA12 (5 wt. %) + C-1 (0.5 wt. %);
6 – PA6.6 (84.5 wt. %) + PA6 (10 wt. %) + PA12 (5 wt. %) + CNT (0.5 wt. %);
7 – PA6.6 (84.5 t. %) + PA6 (10 wt. %) + PA12 (5 wt. %) + UDD (0.5 wt. %)

At the same time, the energy treatment of the surface layer of the product and dispersed particles makes it possible to realize their special structure, which exhibits characteristic signs of nanostate, which determines the achievement of some specific properties, for example, bactericidality [5], which can be used for the manufacture of special-purpose products.

4. Conclusion

The proposed methodological approaches to the creation of composite materials with specified parameters of functional characteristics based on industrially produced thermoplastics make it possible to expand the brand range of composites using traditional manufacturing and processing technologies.

The considered aspects of the mechanisms of formation of the structure of composite materials based on polymer mixtures with different thermodynamic compatibility of components made it possible to develop a range of engineering materials for the manufacture of structural and tribological products and coatings used in the construction of automotive components (cardan shafts, brake chambers, automotive shock absorbers), technological equipment (lathe cartridges), belt conveyors for transportation of bulk and lumpy materials (metal-polymer roller supports), fasteners (dowels), elements of road and building structures (marker posts, curbs, elements of floor and ground coverings) [3, 6].

Regulatory legal and technical documentation regulating the processes of manufacturing and processing of composite materials based on polymer blends with different thermodynamic compatibility of components has been developed.

The developed materials based on industrial thermoplastics of domestic production provide the necessary performance parameters of metal-polymer systems for various functional purposes and are a full-fledged alternative to imported analogues.

Acknowledgments.

The given research was carried out within the framework of integrated assignment 5.6 "Research of the processes of creation and use of polymer packaging materials to ensure the quality and safety of food products" of R&D "Investigation of the processes of structure formation of thermoplastic nanocomposites for obtaining film semi-finished products with increased parameters of characteristics" included in the subprogram “Food security” of the State programs for scientific research “Agricultural technologies and Food security” in 2021-2025.

References

1. Goldade V.A., Struk V.A., Beytyuk Yu.R., Avdeichik S.V., Antonov A.S., (2022). *Engineering and electrotechnical materials*. Minsk, RIVSH, 536 p. (In Russian).
2. Gol’dade V.A., Struk V.A., Pesetskii S.S., (1993). *Wear Inhibitors of Metal Polymer Systems*. Moscow, Khimiya Publ., 240 p. (In Russian).
3. Kravchenko V.I., Kostyukovich G.A., Struk V.A., (2006). *Cardan transmissions: constructions, materials, application*. Minsk, Tekhnalogiya, 410 p. (In Russian).
4. Antonov A.S., (2018). *Composite materials based on thermoplastic blends for increase of service life of technological equipment elements*. Ph.D. in Techn. Sci. thesis, Minsk, 200 p. (In Russian).
5. Avdeichik S.V., Struk V.A., Antonov A.S., (2017). *Factor of nanostate in the materials science of polymer nanocomposites*. Saarbrücken, LAP LAMBERT Asad. Publ., 468 p. (In Russian).
6. Abdurazakov A.A., Avdeichik S.V., Antonov A.S., (2019). Composite materials in the constructions of belt conveyors of increased resource. Tashkent, Vneshinvestprom, 360 p. (In Russian).

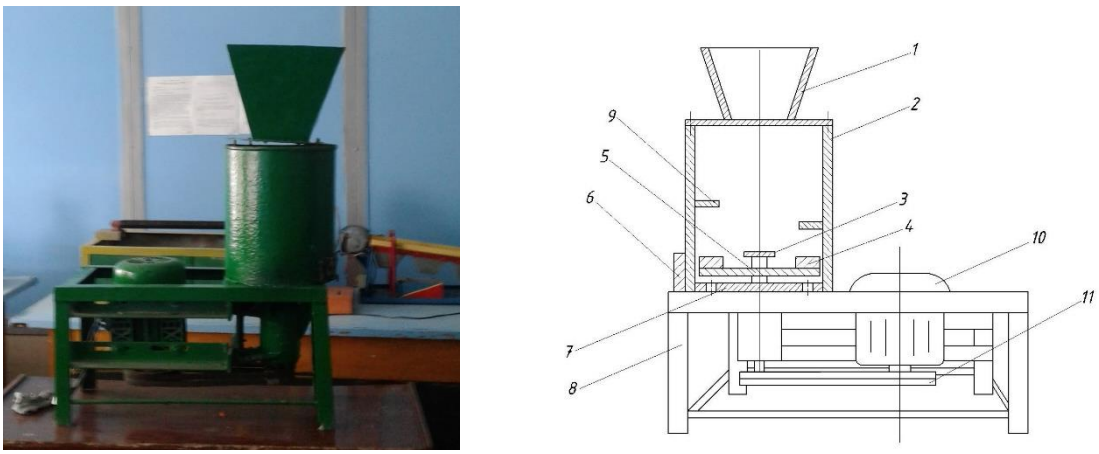
RESULTS OF EXPERIMENTAL STUDIES OF THE PROCESS OF CRUSHING ORGANIC COMPONENTS OF MUNICIPAL SOLID WASTE

Khankelov T.K.[1], Politaeva N. A.[2]
[1]Tashkent State Transport University, Republic of Uzbekistan
[2]Peter the Great St. Petersburg Polytechnic University,
Russian Federation

Abstract. The article is devoted to determining the rational values of the main parameters of a hammer crusher designed for grinding organic waste components. A series of single-factor experiments was performed and a list of factors significantly affecting the grinding process was compiled. Based on the results of a series of experiments, a mathematical model of the process of grinding organic waste components was developed and examined for extremes. The development of a hammer crusher with rational parameter values made it possible to significantly increase the productivity of the crusher.

Keywords: municipal solid waste, hammer crusher, rational parameters, productivity

1. Introduction To substantiate the determining factors, the intervals of their variation, and rational values of the main parameters of the crushing machine, a physical model of the hammer crushing machine was developed and manufactured (Fig. 1).



a) b)

Fig. 1. Hammer crusher: a) general view of the crusher, b) structural scheme of the hammer crusher: 1 - hopper; 2 - working chamber; 3 - rotating knife; 4 -hammer; 5 - rotor; 6 - side grate; 7 - lower grate; 8 - frame crusher; 9 - fixed knife; 10 - electric motor; 11 - V-belt.

The crushing machine consists of hopper 1, which consists of welded steel sheets 1.0 mm thick in the shape of an isosceles trapezoid, the lower ends of which are welded to a disk with a diameter of 300 mm, which in turn serves as the cover of working chamber 2. Working chamber 2 is made of a cast iron pipe with a diameter of 300 mm, the lower end of which is welded to frame 8 of the crusher, and in the upper part of the working chamber four through holes are drilled in a circle, and hopper 1 of the crusher is attached to them with bolts. Electric motor 10 is installed with bolts to frame 8 of the crusher. It is located in such a way that crusher flushing water or liquid waste does not enter the electrical part of the electric motor. To do this, a pulley is installed in the lower part of the working chamber, rigidly mounted on the shaft. A pulley is

attached to the output shaft of electric motor 10 using a key, connected to the pulley of working chamber 2 through a V-belt drive. A cross-shaped working body is mounted on the keys to the upper part of the working chamber shaft. Rotor 5 is welded onto a bushing with a diameter of 20 mm from the lower part, on the outer side of which hammers 4 are welded. Rotating knife 3 is also welded to the upper part of the bushing, the ends of which are sharpened for better grinding. To obtain waste crushed to the required size, side grate 6 is installed in the lower side part of working chamber 2. In addition, to increase the efficiency of grinding organic components of waste in the lower part of the working chamber, lower grates 7 are drilled along the periphery. For better grinding of waste, fixed knives 9 are welded on the walls of working chamber 2 [1; pp.3-7, 2; pp.35-38, 3; pp.8090-8096].

The stand for grinding organic components of solid waste using the hammer crushing machine works as follows. The waste arriving for grinding enters loading hopper 1. Next, the waste enters working chamber 2, where it is accelerated to a rotation speed equal to the rated rotation speed of electric motor 10, due to the creation of air pressure through hammer 4. The waste accelerated to the rated rotation speed of electric motor 10 is crushed due to the collision of waste with knives 9 rigidly welded to the walls of working chamber 2. In addition, the waste is crushed by colliding with grate 5. The sharpened ends of rotating rotors 5 contribute to the effective grinding of waste. Fibrous and film waste is crushed due to abrasion between the lower part of rotor 5 and the bottom of working chamber 2. Due to abrasion, the waste passes through grate 7 located on the bottom of the working chamber [4; pp.274-276, 5; pp.27-33, 6; pp.80-83].

To study the effect of the shape and the angle of installation of hammers relative to the axis passing through the rotor length of the crushing machine on the grinding efficiency, a series of preliminary experiments was performed. Figure 2 shows the designs of rotors with various hammers.



Fig. 2. Designs of rotors with various hammers: a) straight hammers located along the rotor axis; b) hammers located at an angle of 45 degrees to the rotor axis; c) paraboloid hammers.

2. Materials and research methods

The process of crushing the components of solid waste is influenced by many factors, the degree of significance of which varies, especially in the production of mineral fertilizer (compost). In the case of compost production, the crushing machine is equipped with grates. The ranking of factors influencing the crushing process made it possible to determine both primary and secondary factors. To unambiguously determine the crusher rotor parameters, a series of one-factor experiments was conducted to substantiate the shape, mass, and angle of installation of hammers relative to the rotor axis, and to study the effect of waste moisture content on the

productivity of the crushing machine. Figure 3 shows the dependence of crusher productivity on the shape of hammers at different values of the driving power of the crushing machine.

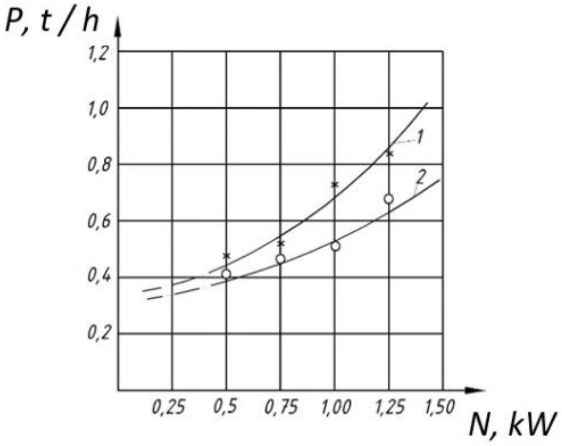


Fig. 3. Dependence of crusher productivity on the shape of rotor hammers at different values of the driving power of crushing machine:
1 - straight shape of the hammer; 2 - paraboloid shape of the hammer

Analysis of the graphs presented in Fig. 3 shows that the productivity of the crusher increases with an increase in the power of the electric motor; however, with a straight shape of hammer (line 1) the growth is more intensive than in the case of a paraboloid shape of the hammer (line 2). The reason for this discrepancy is the following: with a straight hammer, the impact on the components is direct, that is, all the impact energy is applied to the waste components; besides, due to the shape of the blade, the waste components hit a large light surface. With the paraboloid shape of the hammer, first, a concentrated blow is obtained; and second, due to the small distance, there is no noticeable dispersion of the flying components, thus the productivity of the crusher is relatively low. In addition, in the case of a paraboloid shape, electricity consumption will increase due to increased resistance. It was also established that when the driving power of the crusher is less than 0.5 kW, there is a lack of the driving power; this is explained by the fact that the existing moisture content of the waste prevents the rotation of the crusher rotor, and the crushing process does not occur.

To study the dependence of the hammer crusher productivity on the moisture content of solid waste components at different values of the driving power of the crusher, a series of single-factor experiments was performed. Figure 4 shows the dependence of the productivity of a hammer crusher on the moisture content of organic components of the waste at different values of the driving power.

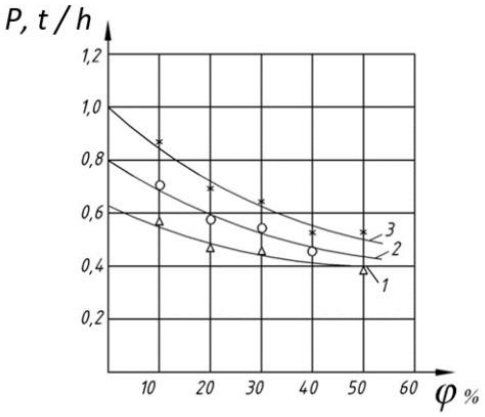


Fig. 4. Dependence of the productivity of a hammer crushing machine on the moisture content of waste components:
1 – for the driving power of the crushing machine equal to 1.0 kW; 2 - for the driving power of the crushing machine equal to 1.25 kW; 3 - for the driving power of the crushing machine equal to 1.5 kW.

Data from literary sources and the results of experimental studies to determine the physical properties of waste over 3 years (depending on seasons) showed that the moisture content of waste varies within 20-50%.

Analysis of the graphs presented in Fig. 4 shows that there is a functional relationship between the productivity and the driving power of a crushing machine; this relationship is relatively close to linear, with fixed values of some parameters that affect the grinding process. As the driving power of the crusher increases, productivity also increases.

The issue of sufficient driving power to achieve maximum performance for specific values of the main design and technological parameters is relevant.

To establish rational values for the diameter of the grate opening, which provides the required linear size of crushed waste components, regulated by compost production, a series of one-factor experiments was also conducted. The dependence of the productivity of the crushing machine on the diameter of the grate (the shape of the hammer is a plate of constant thickness) was determined. Figure 5 shows the dependence of the productivity of a hammer crusher on the driving power, for different values of the grate diameter.

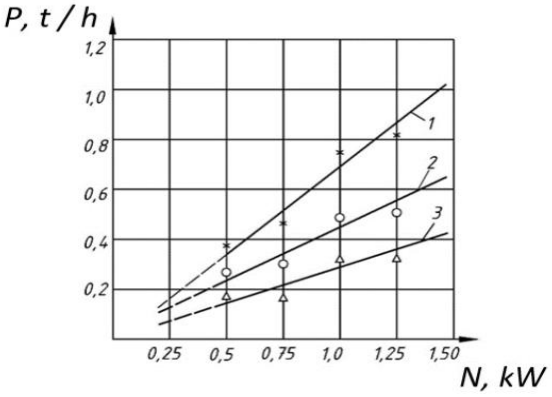


Fig. 5. Dependence of the productivity of a hammer crusher on the dri**ving power for different values of the grate diameter:**

1 - for a grate diameter of 25 mm; 2 - for a grate diameter of 20 mm; 3 - for a grate diameter of 15 mm.

When the driving power of the hammer crushing machine is from 0.25 to 0.5 kW, partial jamming of the rotor occurs due to lack of power, and when the driving power of the crushing machine is 1.5 kW, the productivity of the crushing machine is approximately 1.0 t/h. The relatively low productivity value is due to the fact that the holes in the grates are partially clogged (line 1). When the driving power of the hammer crusher is from 0.25 to 0.5 kW, the grate holes are also clogged, but the relatively small difference lies in the sizes of holes (lines 2 and 3), and when the driving power of the hammer crusher is 1.5 kW, the productivity of the crushing machine is approximately from 0.8 to 0.95 t/h. The maximum value is obtained when the diameter of the grate hole is 25 mm. The disadvantage of this case is that the bulk of the crushed waste has a size of approximately 15-20 mm, which, in turn, does not meet the technical regulations for compost production.

Consequently, to obtain the size of crushed waste within 10-15 mm, a second stage of grinding is required, which leads to significant energy consumption. Therefore, the use of grates with a diameter of 15 mm completely covers such a minor difference in performance due to energy savings. Figure 6 shows the dependence of the productivity of a hammer crushing machine on the driving power of the hammer crusher, at different values of the angle of installation of the rotor hammer.

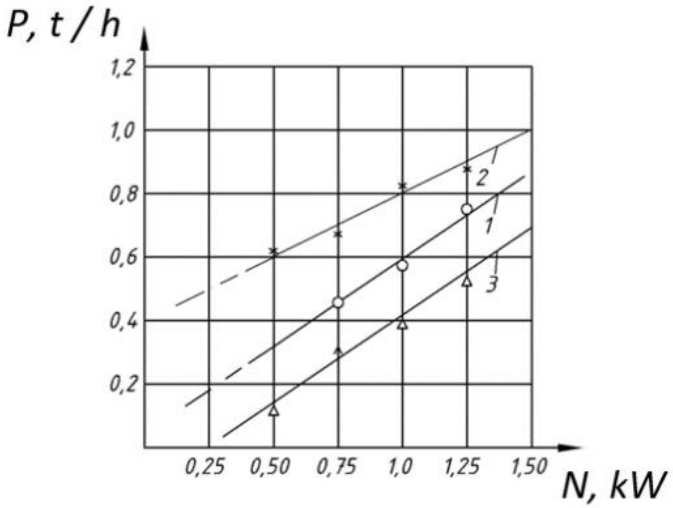


Fig. 6. Dependence of the productivity of a hammer crushing machine on the driving power of the hammer crusher (at different values of the angle of installation of the rotor hammer):

1 - for an angle of hammer installation $\alpha_м = -45^0$; 2 - for an angle of hammer installation $\alpha_м = 0^0$; 3 - for an angle of hammer installation $\alpha_м = 0^0$.

When the driving power of a hammer crushing machine is from 0.25 to 0.5 kW, the rotor shaft jams due to the lack of the driving power to overcome the resistance that arises from the waste components and static resistance forces. The best values are obtained when the hammer installation angle is $\alpha_м = 0^0$ (line 2). This is explained by two reasons: first, when the hammer installation angle is zero, a good pressure force is generated in the working chamber, due to this, the waste components are accelerated to speeds equal to the nominal value of the rotor rotation speed. Obviously, the greater the speed of impact of the components on the wall of the crushing

chamber of the machine, the greater the impact force; the data obtained confirms this fact; second, when the hammer installation angle is zero, a direct impact on the waste components occurs. This is the reason for the collision of waste components against the walls of the working chamber with maximum force. In addition, when the hammer installation angle is zero, the "angle of fire" from the side of the hammer to the grate is the greatest. When the hammer installation angle is $\alpha_м = -45^0$ (line 1), an oblique impact occurs on the waste components, i.e. the impact force is dissipated, thereby the waste components collide with the walls of the working chamber of the hammer with less force. In addition, at an installation angle of $\alpha_м = -45^0$, the air pressure used to speed up the waste components is small.

When the hammer installation angle is $\alpha_м = 45^0$ (line 3), an oblique impact on the waste components also occurs, i.e. the impact force is dissipated, thereby the waste components collide with the walls of the working chamber of the hammer with little force. In addition, at an installation angle equal to $\alpha_м = 45^0$, the air pressure used to speed up the waste components is small. Another important circumstance is that with an installation angle of 45^0, the "angle of fire" on the grate from the side of the hammer is the smallest.

To study the influence of the hammer mass on the crushing process and to determine the intervals of their variation, a series of one-factor experiments was conducted.

Figure 7 shows the graph of the dependence of the productivity of a hammer crushing machine on the driving power (with hammer weights $m_м$ =1.0; 1.2; 1.4 kg). Hammers are rectangular plates of constant thickness. In the experiments, only the width of the hammer changed while the height remained constant.

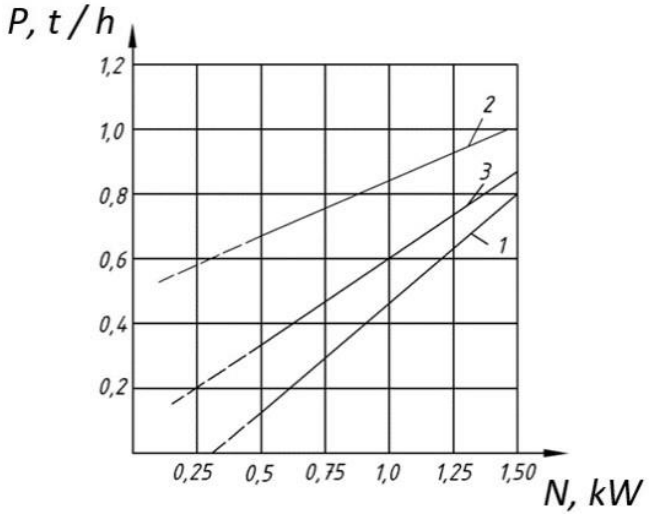


Fig. 7. Dependence of the productivity of a hammer crusher on its driving power at different values of the mass of the hammer: 1 - rotor hammer mass $m_м$=1.0 kg; 2 - rotor hammer mass $m_м$=1.2 kg; 3 - rotor hammer mass $m_м$=1.4 kg.

Analysis of the graphs presented in Fig. 7 shows that when the driving power of the crushing machine is from 0.25 to 0.5 kW, the rotor shaft jams due to the lack of the driving power to overcome the resistance forces that arise from the waste components and static resistance forces. The graphs show that productivity is greatest when the hammer mass is $m_м$=1.2 kg. This is expressed in that, first, an increase in the mass of the hammer helps to

increase the pressure force generated by the hammers, this, in turn, helps to increase the impact force of the waste components on the walls of the working chamber of the crusher; second, an increase in the linear dimensions of the hammer, i.e., the area of contact with waste components increases the "angle of fire" of the grate from the side of the rotor hammer. The reason for the relatively low productivity of a hammer crusher with a hammer mass of $m_м$=1.4 kg is the increase in resistance forces from the air medium and waste components.

An assessment of the dependencies shown in Figures 2-7 indicates that the highest percentage of grinding of organic waste components is achieved:

- for the size of the grate opening approximately D_p ≈15 mm;
- at an angle of installation of the rotor hammer approximately equal to $\alpha_м$ ≈0 degrees;
- for a rotor hammer mass of approximately $m_м$≈1.2 kg.

Data from a priori information and several installation experiments conducted made it possible to clarify the factors that significantly affect the performance of the crushing machine at fixed values of the following parameters:

- rotor shaft rotation speed, n_p, rpm;
- light area of the grate, F_c, cm^2;
- rotor diameter, D_p, cm.

To determine the range of variation of factors and ranking factors by importance, a series of single-factor experiments was conducted.

Figure 8 shows the dependence of the productivity of a hammer crushing machine on the driving power at various values of the rotor shaft rotation speed.

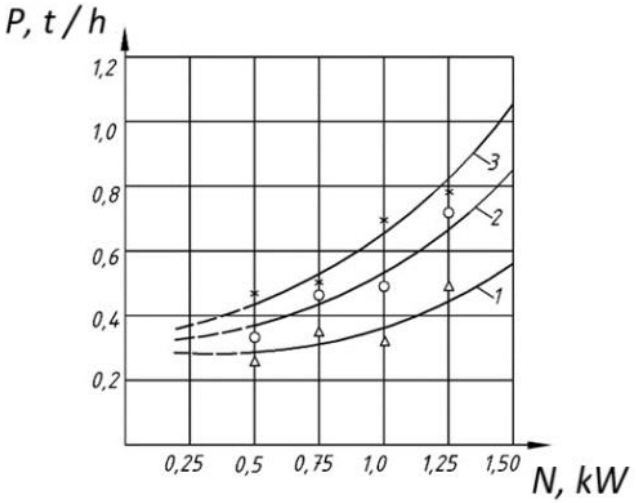


Fig. 8. Dependence of the productivity of a hammer crushing machine on the driving power at different values of the rotor shaft rotation speed: 1- at a rotor shaft rotation speed of n_p=1250 rpm; 2 - at a rotor shaft rotation speed of n_p=1750 rpm; 3 - at a rotor shaft rotation speed of n_p=1500 rpm.

Analysis of the graphs presented in Fig. 6 shows that when the driving power is in the range from 0.25 to 0.5 kW, the rotor shaft jams due to the lack of power to overcome the resistance forces that arise from the waste components and static resistance forces.

As seen from the graphs, the highest productivity value is achieved at a rotor shaft speed of n_p=1500 rpm, which corresponds to the nominal speed of the electric motor rotor shaft. In

addition, when the rotor shaft rotation speed is n_p=1500 rpm, the specific energy intensity is minimal.

At values of rotor shaft rotation speed equal to n_p=1750 rpm (line 3) and n_p=1250 rpm (line 1), the crushing machine has a higher specific energy intensity. In addition, an increase in rotation speed leads to a decrease in torque, as a result of which the performance value decreases. At n_p=1250 rpm (line 1), the waste components will not be able to acquire the speed required for effective grinding. Figure 9 shows the dependence of the productivity of a hammer crushing machine on the driving power for various values of the light area of the grate.

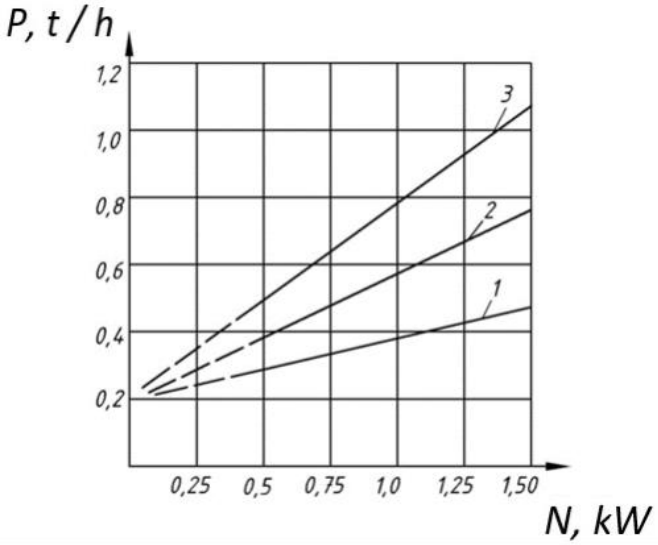


Fig. 9. Dependence of the productivity of a hammer crushing machine on the driving power at different values of the light area of the grate: 1 – for the value of the light area of the grate F_c =250 cm^2; 2 - for the value of the light area of the grate F_c =350 cm^2; 3 - for the value of the light area of the grate F_c =300 cm^2.

The best performance values coincide with the value of light area equal to F_c=300 cm^2 (line 3). The reason for the relatively low productivity value of the hammer crushing machine at F_c= 350 cm^2 (line 2) is explained by the fact that the crushed waste begins to scatter in different directions, polluting the environment, and when installing the unloading device, the periphery of the internal part is clogged with waste and the productivity value is low.

Figure 10 shows the dependence of the productivity of a hammer crushing machine on thebdriving power at various values of the rotor diameter.

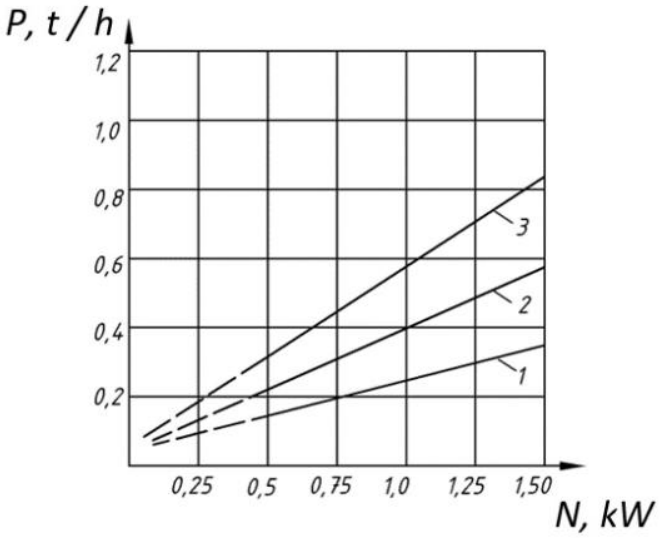


Fig. 10. Dependence of the productivity of a hammer crushing machine on the driving power for different values of the rotor diameter: 1 - for rotor diameter D_p = 24 cm; 2 - for rotor diameter D_p= 27 cm; 3 – for rotor diameter D_p= 30 cm.

Analysis of the graphs presented in Fig. 8 shows that for D_p = 30 cm (line 3), the productivity of the crushing machine has the best values; this is explained by the fact that at this value of the rotor diameter, there is no influence of boundary conditions, i.e. there is a complete coverage of the waste mass located at the wall of the working chamber. Complete coverage of the waste mass allows the maximum value to be achieved. In the other two cases, there is an effect of boundary conditions, when the waste mass pressed against the wall has zero speed, which results in a low productivity value.

Based on the methods of mathematical statistics, by preliminary distribution, considering the review and the results obtained conducting one-factor experiments, the main factors determining the grinding process were established. The dependence of crushing machine performance on the main parameters of the process in implicit form has the following form:

$$Y = f(n_p, F_c, D_p) \quad (1)$$

where n_p is the number of revolutions of the rotor shaft, rpm; F_c is the light area of the grate, cm^2; D_p is the diameter of the rotor shaft, cm; Y is the productivity of the crushing machine, kg/h.

The implicit relationship between optimization factors and parameters is

$$Y = a_0 + \sum a_i x_i + \sum a_{ij} x_{ij} + \sum a_i x_i^2, \quad (2)$$

where Y is the value of the optimization index under consideration; x_i is the coded value of factors (i=1,2,3), a_i is the value of the coefficient characterizing the contribution of the *i*-th factor; a_{ij} is the value of the coefficient characterizing the interaction of factors.

The experiments were conducted according to the Box-Behnken design (B_3) [7; pp.17-192, 8; p.241-247], they considered the complex interaction of factors. Box-Behnken design is the best system and it contains the least sensitivity of coefficient results. In addition, factor variation at three levels provides the necessary accuracy of results at the smallest points of the design. To control the feasibility of the experiments, the Cochran test was used to evaluate the hypothesis of the similarity of variance values with identical repetitions, and the role of the empirical coefficients of the regression equation was assessed using the Student's test with an

accuracy level of 0.05. The ability to depict the response surface quite well, i.e., the conformity of the adopted model was checked using standard methods.

$$F_{\text{рас}} < F_{\text{табл}}, \quad (3)$$

Table 1 shows the factors, their levels, and their ranges of variation.

Table 1. Levels of factors and ranges of their variation

№	Factors	Code	Factor levels			Range	Size
			-1	0	+1		
1	Rotor shaft speed	X_1	1250.0	1500.0	1750.0	250.0	rpm
2	Light area of the grate	X_2	250	300	350	50	cm^2
3	Rotor shaft diameter	X_3	24	27	30	3	cm

A mathematical model of the performance of a prototype crushing machine was obtained based on experimental data and verification of the importance of regression coefficients.

$$Y = 89{,}2 + 7{,}4X_1 - 3{,}4X_2 + 2{,}7X_3 + 3{,}3X_1^2 - 2{,}4X_2^2 + 1{,}8X_3^2 \quad (4)$$

Assessment of model compliance using the Fisher criterion showed that the mathematical model is adequate with 95% accuracy

$$F_{\text{рас}} = 0{,}95, F_{\text{табл}} = 2{,}36\ , \quad (5)$$

To find the best values of the factors, equation (4) was examined to the maximum, the results are given in Table 2.

Table 2. Rational values of factors

Factor values	Factors		
	$X_{1,\text{ mm}}$	$X_{2,\text{ degree}}$	$X_{3,\text{ kg}}$
Coded	0	0	+1
Natural	1500.0	300	30
Rounded	1500.0	300	30

Thus, the best values for the main parameters of the crushing machine are:
- rotor shaft rotation speed n_p ≈1500 rpm;
- light area of the grate F_c ≈300 cm^2;
- rotor diameter D_p ≈30 cm.

3. Conclusions

1. A mathematical model was developed that allows us to determine the rational values of the design and technological parameters of machines that ensure the efficiency of the process of grinding municipal solid waste.

2. The study of a mathematical model of the process of grinding organic components made it possible to substantiate the rational values of a hammer crusher:

- rotor shaft rotation speed n_p ≈1500 rpm;
- light area of the grate F_c ≈300 cm^2;
- rotor diameter D_p ≈30 cm.

3. Grinding the organic components of waste in a hammer crusher with rational parameters will increase the productivity of waste grinding by 25-30%.

References

1. Khankelov T.K., Tursunov Sh.S., Eshnazarova L.G., Nishanov A.A., (2018). Mathematical model of the process of crushing municipal solid waste, *TADI Bulletin*, (4), 3-7.
2. Khankelov T.K., Tursunov Sh.S., (2018). Development of similarity criteria for physical modeling of the process of crushing municipal solid waste, *TADI Bulletin*, (4), 35-38.
3. Maksudov, Z., Kudaybergenov, M., Kabikenov, S., & Sungatollakyzy, A. (2021). The machines optimal set development for the construction of automotive roads elements based on the" Norm" for machines employment cost. In *E3S Web of Conferences* (Vol. 264, p. 02031). EDP Sciences.
4. Khankelov, T., Maksudov, Z., Mukhamedova, N., & Tursunov, S. (2021). Crushing and screening complex for the production of compost from organic components of municipal solid waste. In *E3S Web of Conferences* (Vol. 264, p. 01026). EDP Sciences.
5. Khankelov, T., Askarkhodzhaev, T., & Mukhamedova, N. (2020). Determination of key parameters of a device for sorting municipal solid waste. *Journal of Critical Reviews*, *7*(4), 27-33.
6. Dixon, N., & Jones, D. R. V. (2005). Engineering properties of municipal solid waste. *Geotextiles and Geomembranes*, *23*(3), 205-233.
7. Adler Yu, P., Markova, E. V., & Granovsky Yu, V. (2003). Planning an experiment when searching for optimal conditions.
8. Augambaev, M., Ivanov, A. Z., Terekhov, Y. I., & Rudakova, G. M. (1993). Fundamentals of planning a research experiment. *Tashkent: "Uqituvchi*.